Concentrated Solar Power techno-economic analysis in humid subtropical South America. The Uruguayan case.

Agustín Ghazarian[1], Pedro Galione[1,*], Pedro Curto[1]

[a]*Facultad de Ingeniería, Universidad de la República, Julio Herrera y Reissig 565, 11300, Montevideo, Uruguay*

Abstract

This study assesses the feasibility of installing concentrated solar power plants in subtropical South America, particularly in Uruguay, by numerical simulations. Parabolic Trough and Solar Power Tower technologies are examined. A comprehensive literature analysis is conducted in order to evaluate initial investment, operation, and maintenance costs. Simulation models are validated in order to ensure results accuracy. The study is focused on the optimization of solar fields and storage sizes for five locations. The target set is to minimize the Levelized Cost of Energy. In addition, energy losses and efficiencies are compared between Parabolic Trough and Solar Power Tower technologies. Salto region in Uruguay is identified as the most suitable location for Concentrated Solar Power projects. Optimized plants yield solar multiples of 3 or higher for Solar Power Tower and around 4 for Parabolic Trough, with storage sizes ranging from 12 to 15 hours, depending on the location. In Salto, the Levelized Cost of Energy ranges from 148 to 175 USD/MWh for 110 MW Solar Power Tower and from 169 to 220 USD/MWh for 55 MW Parabolic Trough plants, considering different investment cost scenarios. Levelized Cost of Energy is comparable for other locations, with a slight increase of approximately 10% for the least favorable location, Rocha. This work shows that while not yet competitive with photovoltaic or wind technologies, concentrated solar power plants show promise

*Corresponding author

against fossil-fueled power plants and are expected to decrease further in cost.
Keywords: Concentrating Solar Power, Levelized Cost Of Energy, Thermal Energy Storage, Modeling and Optimization

Concentrated Solar Power techno-economic analysis in humid subtropical South America. The Uruguayan case.

Agustín Ghazarian[1], Pedro Galione[1,*], Pedro Curto[1]

[b]*Facultad de Ingeniería, Universidad de la República, Julio Herrera y Reissig 565, 11300, Montevideo, Uruguay*

NOMENCLATURE

Latin symbols:

E	energy (MWh, GWh)
i	discount rate
I	investment (USD, MUSD)
$LCOE$	levelized cost of energy (USD/MWh)
M	Operation and maintenance costs, including taxes (USD, MUSD)

Superscripts and subscripts:

a	year

Abbreviations:

*Corresponding author

Preprint submitted to Journal of Solar Energy Engineering *April 16, 2024*

BOP	Balance Of Plant
CF	Capacity Factor
CSP	Concentrated Solar Power
DNI	Direct Normal Irradiance
HTF	Heat Transfer Fluid
I.I.	Initial Investment
IRAE	economic activity income tax (Uruguay)
MBD	Mean Bias Deviation
NREL	National Renewable Energy Laboratory (USA)
O&M	Operation and Maintenance
OPEX	Operating Expenses
OE	Optical Efficiency
PT	Parabolic Trough
RMSD	Root Mean Square Deviation
SAM	System Advisor Model
SPT	Solar Power Tower
TIC	Total Investment Cost
TMY	Typical Meteorological Year

1. Introduction

Concentrated solar power (CSP) technologies are a renewable alternative for producing electricity or heat that, unlike wind and photovoltaic technologies, can easily incorporate thermal storage. These power plants were initially implemented mostly in the United States and Spain, but China and Morocco have recently emerged as major investors [26]. The global CSP installed capacity at the end of 2021 was around 6.4 GW, having increased five-fold in 10 years [16].

In the last few years, and mainly due to China's insertion into the market, Levelized Cost of Energy (LCOE) of CSP has dropped significantly, together with an increase in capacity factors [17, 16] (see Table 1). The decrease in storage costs is a critical component in the progress of technology, making large-size storage capacities possible and therefore improving the capacity factor of the plants [14]. Although the presented energy prices are far from competitive with other renewable technologies [16], the situation is relatively hopeful when compared to fossil fuel power plants.

Good irradiance is critical for these technologies to be competitive. According to Islam et al. [17], viable CSP plants should be located in areas with Direct Normal Irradiance (DNI) values of at least $2000\frac{kWh}{m^2 year}$. In humid subtropical South America (Köpen climate classification Cfa) —a region comprising north-eastern Argentina, Uruguay, southern Paraguay, and southern Brazil— annual DNI values are close to this threshold but somewhat lower for most locations. In particular, available DNI in Uruguay ranges between 1740 to $1900\frac{kWh}{m^2 year}$ [2]. Therefore, being lower to the limit of considered viability, it is interesting to analyze this viability in more detail.

The Solar Energy Laboratory in Uruguay has been working on the development of a reliable database of solar irradiance. Moreover, the above-mentioned laboratory created a Typical Meteorological Years (TMY version 2.4) for solar applications, for five locations in Uruguay (shown in Figure 1). Parameters such as hourly Direct Normal Irradiance (DNI), ambient temperature, pressure, and wind velocity data [2] are presented. A brief summary of some of these parameters is exposed in Table 2. Salto (north of the country) appears to be the best location for a solar project, with a relatively high DNI comparable to that of several locations in Spain where CSP units have been erected.

Several CSP plant feasibility studies have been published recently (see e.g. [7, 9, 25, 4, 3, 5, 12, 10]), mainly in the Middle East and North Africa region. Most of them use Solar Advisor Model (SAM) as the modeling software. In South America, Dos Santos et al. [9] study the feasibility of both SPT and PT plants located in Brazil. Despite being located in South America, in a Brazilian location close to the Equator (Bahia) with a value of DNI of around $2100\frac{kWh}{m^2 year}$, they present quite high values of LCOE (higher than 500 USD/MWh), probably due to a significantly lower economic study period. In the rest of the referenced works, LCOE values as low as 45 USD/MWh [25] and as high as

Figure 1: Locations in Uruguay where Typical Meteorological Year is available (extracted from [2]). COL: Colonia; MVD: Montevideo; RIV: Rivera; ROC: Rocha; SAL: Salto.

220 USD/MWh [5] or even 259 USD/MWh [4] (this last value for cases with a high interest rate on debt) are found. The places where these works are focused have a higher radiation level than that available in Uruguay. Apart from the solar resource (DNI), it is clear that financial parameters affect LCOE significantly.

The potential of CSP technology in Uruguay has only been evaluated in a prior study conducted by SOLIDA Energías Renovables [29], a private consulting organization. They employed an in-house non-free physics-based software as the simulation tool. Detailed piping and instrumentation diagrams ($P\&ID$) are available in [29]. Different configurations were studied, considering both PT and SPT technologies, with maximum storage capacities of 7.5 and 10 hours, respectively. The resulting LCOE values for plants located in Salto were 142 €$/MWh$ for 100 MW SPT and 182 €$/MWh$ for 50 MW PT. A preliminary version of the TMYs was used in that work.

Several computational models are available for CSP simulation, as has been observed by Clifford et al. [13]. They present an analysis of those models indicating their respective applications, strengths, and weaknesses. Only four of the many codes shown are “total performance models”, that is, models in

Table 1: Solar Power Tower (SPT) technology total investment cost (TIC) and capacity factor (CF) for several places across the world[26].

	TIC (USD/W) 110 MW		CF	
	Minimum	Maximum	Minimum	Maximum
North America	6.65	8.08	0.27	0.52
Asia	3.18	7.79	0.21	0.54
Europe	6.24	9.35	0.23	0.41
Africa	5.71	7.20	0.34	0.36
Middle East	6.49	6.97	0.24	0.39
Oceania	6.96	6.96	0.11	0.23

Table 2: Annual direct normal irradiation, mean ambient temperature for some locations in Uruguay [2]

	Latitude (°)	Longitude (°)	Direct Normal Irradiation (kWh/m^2yr)	Temperature (°C)
Colonia	-34.5	-57.8	1890.3	16.6
Montevideo	-34.8	-56.0	1862.5	16.5
Rivera	-30.9	-55.5	1779.7	18.4
Rocha	-34.5	-54.3	1740.6	16.2
Salto	-31.3	-57.9	1897.5	19.3

which overall performance metrics are derived from input data (geometry, solar radiation, temperature, and so on). These are DELSOL, SAM, SOLERGY, and TRNSYS.

In the present work, SAM is selected due to its reliability, simple interface, available documentation, ability to model SPT and PT technologies, ability to run economic analyses, plant characteristics database size, free access, and low computational requirements. Due to its main influence on economic feasibility, an extensive investigation of investment costs is carried out. Furthermore, CSP plants are simulated in five distinct locations, and an optimization of the solar field and storage size is carried out in order to minimize the LCOE. Finally, for the optimized configurations of both SPT and PT plants, energy performance and efficiency parameters are analyzed and compared.

2. Methodology

This section explains in some detail the procedure followed for modeling both concentrated solar power technologies as well as the approach in order to obtain the Levelized Cost of Energy.

The software used for the numerical simulation is the System Advisor Model (SAM) [23]. The System Advisor Model (SAM) is a software tool developed by the National Renewable Energy Laboratory (NREL) in the United States. It is widely used for the design and analysis of renewable energy systems, particularly solar energy systems. SAM provides a comprehensive set of tools and models that allow users to evaluate the performance, feasibility, and economic viability of various renewable energy technologies.

The Typical Meteorological Year (TMY) is utilized for the mentioned five different locations to incorporate radiation data, ambient temperature, wind speed, and other pertinent meteorological information [2].

This section is divided into four subsections: 1) Solar Power Tower model, 2) Parabolic Trough model, 3) Model validation, and 4) LCOE evaluation.

2.1. Solar Power Tower Model

The initial stage in designing the SPT system involves determining the direct normal irradiance (DNI) present at the design point, along with the desired solar multiple (the ratio of receiver thermal power to cycle thermal power). More information can be found in [31]. Additionally, the design must take into account the nominal hot and cold heat transfer fluid temperatures at design conditions, as well as the required storage size, design turbine gross output, estimated gross-to-net efficiency, and power cycle thermal efficiency. Based on the provided information and the geometrical properties of the heliostats (width, height), the Solar Power Tower Model generates an optimal layout of the heliostat field and assesses its optical performance.

The tower height, receiver dimensions, and heat transfer properties are essential requirements. A comprehensive thermal model is utilized for the receiver, which involves solving the energy balance for each time step. This model accounts for multiple heat transfer mechanisms, such as incident radiation, external convection, and radiation exchange with the surroundings.

The common parameters for all the SPT cases are presented in Table 3. It is important to note that the heliostat area is chosen based on SOLIDA [29], while the remaining parameters are set to typical SAM values [23]. In the LCOE optimization process, the number and configuration of heliostats, tower height and receiver dimensions are modified, together with the storage size. The tower, receiver and field configurations are optimized by SAM using the SolarPILOT module [24] with design parameters provided by default, such as the maximum receiver flux ($1000\,kWt/m^2$). The power cycle gross efficiency shown corresponds to a nominal value at design conditions. SAM uses this value to calculate the "real" gross power cycle efficiency for each time step, considering changes in heat transfer fluid inlet temperature and mass flow (e.g. in part-load conditions), as well as ambient temperature (affecting condenser pressure) [32, 24]. The nominal value adopted here is similar to that presented in [29] and is chosen to obtain net generated energy results similar to those presented there.

Further details regarding the configurations under consideration can be found in [11].

Table 3: Solar Power Tower technology specifications.

Gross power output	110 MW
HTF† inlet/outlet temperature	287.8°C/565.6°C
Tower height* (SOLIDA)	180 m
Tower height (optimized)*	$\sim$ 225 m
Receiver area (optimized)*	$\sim$ 1400 m^2
Heliostat area	66.1 m^2
Turbine inlet pressure	100 bar
Cycle thermal nominal gross efficiency‡	43.9%
HTF†	Molten salt
Condenser cooled by air	

* Approximate values for optimized cases presented in section 3.1
† Heat Transfer Fluid
‡ Estimated using data from [29]

2.2. Parabolic Trough Model

SAM provides two alternative options for sizing the solar field in PT. The user has the choice to define either the solar multiple or the solar field aperture. Additionally, specific parameters such as row spacing, collector orientation, and number of collectors per loop must be specified [32].

Multiple models of collector mirrors are accessible, each with its corresponding reflective aperture, length, tracking error, reflectance, and cleanliness factor. Additionally, there is a receiver library that compiles geometric and optical details for a diverse range of receivers. Finally, it is necessary to define the gross output of the power cycle design, the estimated gross-to-net conversion factor, thermal efficiency, and storage size. Reference values are provided for each field.

Table 4: Parabolic trough power plant specifications.

Gross power output	55 MW
HTF† inlet/outlet temperature	293°C/393°C
Turbine inlet pressure	100 bar
Cycle thermal nominal gross efficiency‡	35.6%
Receiver	Schott PTR70
Collector	SkyFuel/Trough
Length of collector assembly	150 m
Number of modules per assembly	12
HTF†	Therminol-VP-1
Condenser cooled by air	

† Heat Transfer Fluid
‡ Default value from SAM

For the case studies involving a typical parabolic trough power plant, the adopted nominal parameters are presented in Table 4. In this case, the adopted gross power cycle efficiency value corresponds to the default value suggested in SAM. More information is available in [11].

The geometric parameters (such as reflective aperture area, aperture width, length of collector assembly, etc.) were chosen to align with those found in the SOLIDA report [29]. The remaining parameters were set based on typical values provided by SAM [23]. Therminol VP-1 is used as the thermal fluid. SAM calculates the necessary properties automatically.

2.3. Validation

SAM power tower and parabolic through models are compared against the results exposed by Solida [29]. For PT, a comparison against an in-house model [11] is also performed. In [29], six configurations are analyzed for each technology (varying solar field and storage size). Since that work was developed in 2014, an older version of the Typical Meteorological Year (TMY 1.0) was employed. In order to minimize the uncertainties, the same TMY version was employed for comparison, only in the validation analyses.

2.3.1. Solar Power Tower model validation

The different configurations presented in the SOLIDA [29] report are adopted here (with the specifications shown in Table 3), involving six different sets of sizes for the solar field and the storage system. These, as well as the annual energy generated by each one, are presented in Table 5.

Table 5: 110 MW SPT plant configurations used in [29]. Comparison of annual generated electricity (GWh$_e$).

SPT 110 MW				
Number of heliostats	Storage hours	SOLIDA GWh$_e$	SAM GWh$_e$	Differences (%)
16770	5	320.8	320.6	-0.06
18295	5	328.2	329.1	0.27
18295	7.5	364.9	361.3	-1.00
19819	7.5	373.2	373.7	0.13
19819	10	398.6	398.2	0.10
21343	10	408.8	410.7	0.47

A remarkable resemblance among the results is evident, resulting in a maximum difference of 1%, an MBD (Mean Bias Deviation) error of 0.04%, and an RMSD (Root Mean Square Deviation) of 0.47%.

2.3.2. Parabolic Trough model validation

The results obtained with SAM are compared here with those reported by SOLIDA [29] (with the specifications shown in Table 4), for each configuration presented in their report (see Table 6), and with those obtained using an internal code (detailed in [11]).

Table 6: 55 MW PT plant configurations used in [29]. Comparison of annual generated electricity (GWh$_e$) against results from [29] and an in-house code.

PT 55MW						
Number of Loops	Storage hours	SOLIDA GWh$_e$	SAM GWh$_e$	SAM Diff. (%)	Own Code GWh$_e$	Own Code Diff. (%)
92	0	84.2	85.9	-2.0	85.3	-1.3
123	0	99.0	97.2	1.9	100.9	-1.9
123	5	123.5	126.0	-2.0	125.0	-1.2
155	5	143.2	144.4	-0.8	143.0	0.1
155	7.5	152.5	156.0	-2.3	154.0	-1.0
186	7.5	168.0	172.0	-2.4	168.7	-0.4

There is a strong consensus among the various results obtained, with no instance showing a difference in the predicted generated energy exceeding 2.5%. When using SAM, the MBD (Mean Bias Deviation) and RMSD (Root Mean Square Deviation) errors are -1.44% and 2.0% respectively. Conversely, when utilizing the in-house code, the MBD and RMSD errors are -0.84% and 1.0% respectively.

2.4. LCOE evaluation

The levelized cost of energy (LCOE) is a crucial parameter that can be optimized for the economic assessment of energy projects. It considers the present value of all project costs over its lifespan and establishes the electricity price required for profitability. The calculation of LCOE involves the utilization of a discount rate (i), which represents the interest rate used to determine the present value of future cash flows.

A study period of 20 years is selected, matching the amortization duration for the power cycle, solar field, heat transfer fluid (HTF) system, and balance of plant (BOP). The initial investment is assumed to occur in year 0, coinciding with the plant's construction, without any profits or reinvestments considered within the study period. The determination of LCOE follows the procedure outlined in Equation 1.

$$LCOE = \frac{\sum_{a=0}^{b=20} \frac{I_a+M_a}{(1+i)^a}}{\sum_{a=1}^{20} \frac{E_a}{(1+i)^a}} \tag{1}$$

where i is the interest rate as defined above; I_a the investment required; M_a indicates operation and maintenance costs (both fixed and variable) as well as taxes, a is each specific year within the 20 years lifetime, and E_a the produced energy in year a. In addition, no degradation is considered, leading to constant energy production throughout the study period. No loan has been considered in this work for financial leveraging.

In Uruguay, energy projects are subject to the IRAE tax, which amounts to 25% of the company's pre-tax utility, after deducting amortizations and depreciation for both tangible and intangible assets. To encourage industries focused on renewable technologies, various benefits are provided, resulting in reduced financial costs. These benefits are determined based on the scoring system outlined in Uruguayan decree 143/018 [30], which assigns points ranging from 1 to 10 across different areas such as job creation, export growth, decentralization, clean technologies, and sector performance. These scores are then weighted by factors specified in the aforementioned decree. Further details can be found in 2.4.3).

Starting with the assumed sizes of the solar field and storage, the annual generated power is obtained from the plant simulation. With an assumption on the energy price (which at the end of the procedure will be equal to the LCOE), the annual income is obtained. The utilities before taxes are derived by subtracting production and depreciation costs, and subsequently applying the corresponding taxes (IRAE) and exoneration for each specific location. Additionally, the depreciation cost is included in the calculation for tax purposes, even though it does not represent an actual expenditure. Finally, the LCOE is obtained using 1. However, as the cost of taxes is dependent on the annual income, an iterative procedure is needed to obtain final LCOE values. Solar field sizes and storage sizes are varied and LCOE for each case is obtained until a minimum value of LCOE is found.

Moreover, a sensitivity analysis is conducted to assess the extent to which variations in initial investment costs and energy production impact the LCOE.

2.4.1. Initial Investment (I.I.)

Ensuring accurate determination of costs is a crucial factor in conducting a thorough analysis of these projects. To achieve this, an extensive literature review was conducted, resulting in the identification of various initial investment costs. These costs, categorized by installed capacity and technology, are detailed in the appendix. Additionally, important project details such as location, available irradiation in the specific area, and storage size are specified to provide comprehensive information.

As presented in the Appendix in Tables 16 to 21 , detailed information is mainly available for projects located in China, leading to initial investment costs of around $5.0\frac{MUSD}{MW}$ for 110 MW Solar Power Tower with 10 or more storage hours and $6.0\frac{MUSD}{MW}$ for 55 MW Parabolic plants at the same storage conditions.

A significant disparity is observed when comparing these projects to those located in other regions (refer to Tables 22 and 23 in the Appendix for comparisons with the USA and Spain, respectively). While the technology learning curve may contribute to this difference (as papers on projects in China tend to be more recent), it appears that the magnitude of the difference cannot be solely attributed to this factor.

Another valuable source of economic data is the System Advisor Model (SAM) provided by the National Renewable Energy Laboratory (NREL). NREL offers comprehensive information specifying costs for each component of the plant, with a specific focus on the solar field and storage size. These costs are taken into account during the optimization process, resulting in costs of $145\frac{USD}{m^2}$ and $24\frac{USD}{MWht}$ for the solar field and thermal energy storage of SPT plants, respectively; and $150\frac{USD}{m^2}$ and $65\frac{USD}{MWht}$ for the PT case. Detailed information can be found in Tables 24 and Table 25 in the Appendix.

To facilitate the comparison with the information provided in Table 16 and 21, a configuration consisting of 23,335 heliostats and a 254-loop power tower and parabolic trough plants, both equipped with a 12.5 hours storage system, is considered.

When comparing the results obtained considering NREL information, of $6.0\frac{MUSD}{MW}$ and $7.9\frac{MUSD}{MW}$ for 100 MW solar power tower and 50 MW Parabolic Trough respectively, to the initial costs obtained from the mentioned papers of $5.0\frac{MUSD}{MW}$ (-16.7%) and $6.0\frac{MUSD}{MW}$ (-24%) a great difference is observed. Due to this factor, two different scenarios are considered for the economic analysis varying the initial investment cost between the values presented.

The Initial Investment costs obtained in this study are compared with the figures presented in [15]. Figure 2 illustrates the progression of initial investment costs categorized by technology and storage capacity. The values obtained in this study are represented for year 2020. It can be observed that the worst-case scenario for PT technology and the initial years of PT power plants exhibit similar values, while the most favorable case aligns with the costs of the latest installed plants. Regarding SPT technology, information before 2014 is unavailable, which can be attributed to its significant advancements occurring in recent years. Nevertheless, both scenarios appear reasonable, with the favorable scenario appearing to align better with the trends observed in 2018 and 2019. Finally, the investment costs utilized in [29] are presented, with the initial investment costs for the optimized SPT and PT power plants, considering storage sizes of 10 hours and 7.5 hours respectively, amounting to 6.2 $\frac{MUSD}{MW}$ and 5.8 $\frac{MUSD}{MW}$, based on an exchange rate of 1.3 Euro-Dollar.

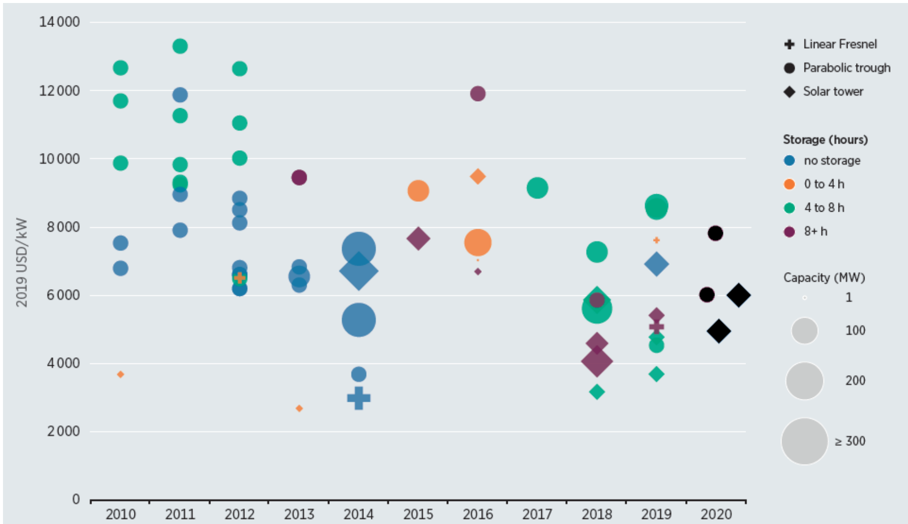

Figure 2: Comparison of initial investment costs in the last decade. Extracted from [15] (©IRENA 2020) and modified to include costs adopted in this work (indicated in black, in the year 2020), for the two considered scenarios.

2.4.2. Operation and maintenance (O&M)

In this study, the operation and maintenance costs provided in SAM [23] are utilized [1]. For both technologies, a fixed O&M cost of 66 $\frac{USD}{kW-year}$ is taken into account. Additionally, the variable operation and maintenance costs for SPT and PT amount to $3.5\frac{USD}{MWh}$ and $4.0\frac{USD}{MWh}$, respectively.

2.4.3. Taxes

Utilizing the procedure exposed in 2.4 the following IRAE exoneration percentage and period is achieved (see Table 7).

Table 10 in section 3 presents the cash flow corresponding to the optimized SPT plant in Salto. It is observed the tax exoneration represents around 2% of the total revenue.

[1]these OPEX costs are valid for the US, but might be different when adapted to the Uruguayan context

Table 7: Tax exemption amount for each considered location in Uruguay.

Location	Exoneration (%)	Exoneration period
Colonia	80.0	20.0
Montevideo	80.0	19.0
Rivera	80.0	20.0
Rocha	80.0	20.0
Salto	80.0	20.0

3. Results

Within this section, the optimization of the solar field and storage size is carried out to achieve the lowest achievable LCOE. The optimal configurations for each technology and location are presented, along with the corresponding achieved LCOE values for the two aforementioned cost scenarios. Furthermore, a comparison is made with the results obtained in [29] to analyze the impact of the optimization process.

To illustrate the influence of initial investment costs and electricity generation on the final outcome, a sensitivity analysis is provided. Additionally, an analysis of the energy performance is carried out, where annual electricity generation for each technology and location is presented, and the different energy losses are compared.

3.1. Optimization

The optimization process involves determining the optimal sizes for the storage and solar field that result in the lowest LCOE value. This optimization is carried out for both technologies and every location where irradiation data is accessible. For SPT, the number and positions of the heliostats were changed as well as tower height and receiver dimensions, to optimize cost and performance.. Figure 3 and Figure 4 illustrate the evolution of LCOE as a function of the mentioned parameters for Power Tower and Parabolic Trough plants, respectively, situated in Salto, representing the worst-case cost scenario.

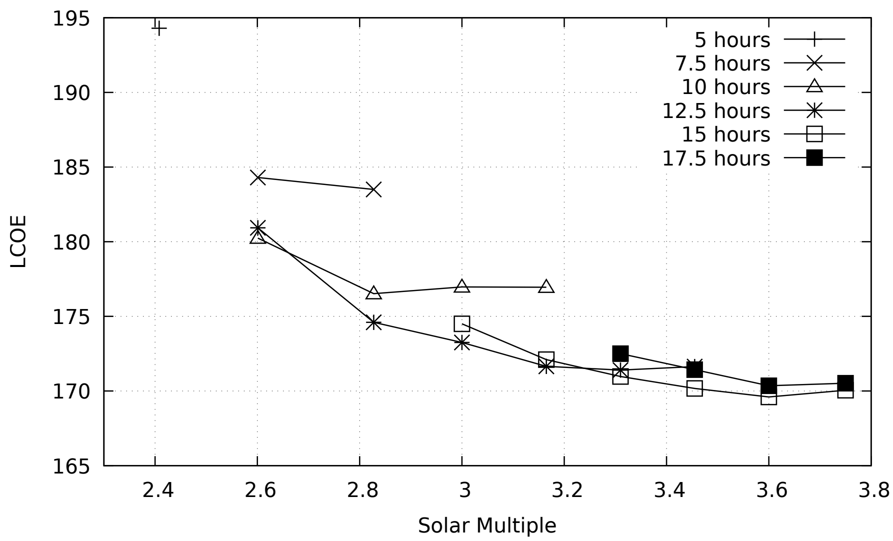

Figure 3: Levelized cost of energy vs solar multiple, for different storage hours. For a SPT technology located in Salto.

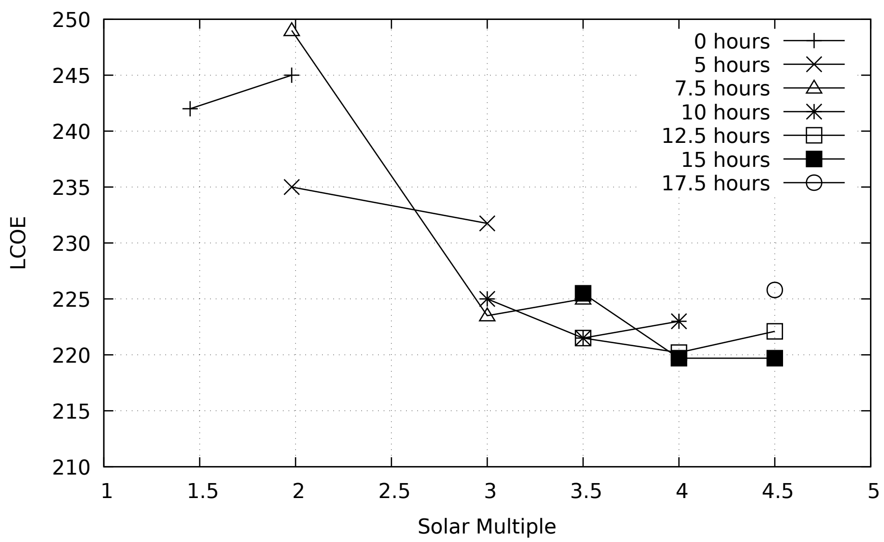

Figure 4: Levelized cost of energy vs solar multiple, for different storage hours. For a PT technology located in Salto.

As depicted in Figures 3 and 4, the LCOE stabilizes within a certain range when the storage sizes range from 12.5 to 17.5 hours and with large solar fields.

In such cases, the chosen criterion is to select the option that requires less capital investment, meaning a smaller solar field and storage size. The optimal configurations for each location under consideration are provided in Table 8 and 9. Furthermore, Table 10 displays the cash flow associated with the optimized SPT plant in Salto.

Table 8: Optimal configuration of a 100 MW SPT plant and its LCOE.

Location	Solar Multiple	Storage size (hours)	LCOE (USD/MWh)
Colonia	3.9	15.0	170.3
Montevideo	3.6	15.0	178.4
Rivera	3.6	15.0	179.2
Rocha	3.6	15.0	189.0
Salto	3.6	15.0	169.6

Table 9: Optimal configuration of 50 MW PT plant and its LCOE.

Location	Solar Multiple	Storage size (hours)	LCOE (USD/MWh)
Colonia	4.0	12.5	220.9
Montevideo	4.0	12.5	227.3
Rivera	4.5	15.0	236.1
Rocha	4.0	12.5	243.7
Salto	4.0	12.5	220.0

Table 10: Cash flow of SPT optimal configuration, in Salto (in millions of dollars, MUSD).

	2021	2022	2023	...	2039	2040	2041
Revenue		83.9	83.9		83.9	83.9	83.9
Production Costs		-9.0	-9.0		-9.0	-9.0	-9.0
Depreciation		-32.4	-32.4		-32.4	-32.4	-32.4
Utility before taxes		42.4	42.4	...	42.4	42.4	42.4
Taxes		-10.6	-10.6		-10.6	-10.6	-10.6
Taxes Exoneration		8.5	8.5		8.5	8.5	8.5
Net utility		40.3	40.3		40.3	40.3	40.3
Depreciation		32.4	32.4		32.4	32.4	32.4
Initial investment	-719.3						
Working capital	-0.75						-0.75
Salvage value							23.6
Total	-719.3	72.7	72.7	...	72.7	72.7	97.1

The same analysis considering the initial investment costs stated in study cases for China is presented in Table 11 for Salto, where in the case of SPT a reduction of 16.7% of the initial investment cost of the optimized plant (6.5 MUSD/MWe) was considered.

Table 11: Investment and LCOE both technologies (STP and PT), considering favorable investment conditions for a location in Salto.

Technology	I.I. (MUSD/MWe)	I.I. Variation (%)	LCOE (USD/MWh)	LCOE variation (%)
Solar Power Tower	5.6	-16.7	143.6	-15.0
Parabolic Trough	6.0	-24.0	168.8	-23.3

Significant differences are evident among the proposed scenarios. In no instance does this technology demonstrate competitiveness compared to photovoltaic or wind power projects, with electricity costs averaging around $40\frac{USD}{MWh}$; although the dispatch capacity of CSP remains a relative advantage of this technology. On the other hand, in the favorable scenario, the attained electricity costs are comparable to those of fossil fuel plants like “Punta del Tigre”(Gas turbines) that operate using diesel as fuel, with costs around $150\frac{USD}{MWh}$ [1].

Lastly, a comparison of the obtained results for both scenarios and technologies is presented in Figure 5. The results here obtained for both technologies tend to be in the lower range of real projects in any region, except China. On the other hand, in some of the previously referenced works (see e.g. [7, 25, 10]), lower values are observed for optimized plants in regions with a better solar resource.

As no loans have been considered for covering part of the initial investment, it is reasonable to expect lower LCOE values if financial leveraging strategies were employed. Additionally, no incentives for selling electricity during peak hours have been considered. If it were possible to sell electricity at variable prices during the day (time-of-day prices), LCOE values could decrease, and optimal plant configurations might vary as the use of thermal storage would be adjusted to prioritize power production during peak consumption periods.

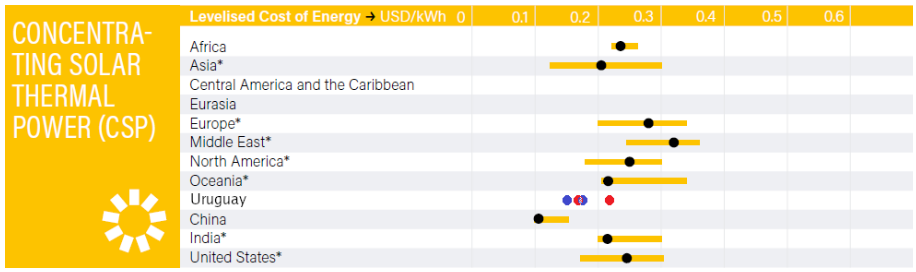

Figure 5: LCOE for some locations in the globe including results of this work for South America (for both scenarios and technologies, SPT in blue, PT in red). Modified from [26].

3.2. LCOE comparison with those reported by SOLIDA [29]

To compare the results obtained with those of the SOLIDA report [29], an inflationary component of 2% is incorporated into the OPEX[2] costs and degradation of electricity generation of 0.2% per year is considered, since these values are adopted in their work. In addition, the amortization and economic analysis are extended to 25 years, as is done in the aforementioned document. It should be noted that some of the calculated benefits, such as the IRAE exemption, are applicable only during the first 20 years. The resulting LCOE and its comparison are presented in Table 12 for both technologies located in Salto.

Regarding the initial investment cost used, the NREL (least favorable) scenario is considered, since no projects had been implemented or studied in China at the time of the publication of the previous work. When considering SPT technology, those reported by SOLIDA [29] are similar to those of NREL (6.2 $\frac{MUSD}{MW}$ and 6.5 $\frac{MUSD}{MW}$, respectively), although the storage sizes differ somewhat (10 hours in SOLIDA [29] and 15 hours for this study). However, for PT technology, there is a significant disparity between the scenarios, with 5.8 $\frac{MUSD}{MW}$ in SOLIDA and 7.9 $\frac{MUSD}{MW}$ in the present study. This difference can be partly explained by the substantial variation in storage system size, with SOLIDA [29] using a storage capacity of 7.5 hours compared to 12.5 hours in this study.

[2]Operating Expenses

Table 12: Levelized Energy Costs (in USD/MWh) for comparison with those of the SOLIDA report [29]. The LCOE values were adapted for the cases of optimized SPT and PT plants (previously obtained), located in Salto, considering the degradation of electricity generation and inflationary effects.

	Previous LCOE	LCOE Adapted	LCOE 25 years	LCOE SOLIDA [29]	LCOE variation (%)
SPT	169.6	172.0	165.7	190.3	-13.0
PT	220.0	226.4	213.9	243.5	-13.8

Although there are some uncertainties regarding the initial investment, a significant decrease can be observed with respect to the results of LCOE presented in SOLIDA [29].

3.3. LCOE sensitivity analysis

A sensitivity analysis is performed considering 5% variations in the initial investment cost (I.I.) and generated energy (E), and evaluating their impact on LCOE. Results are presented in Table 13.

It is evident that each variation produces a similar impact on the resulting LCOE, indicating the dominant influence of these factors over other considerations such as OPEX costs and taxes. This phenomenon suggests that these particular variations have a significant effect, overshadowing the importance of other factors in the overall outcome.

Table 13: Levelised Cost Of Energy sensitivity analysis for optimized plant in Salto, for SPT and PT plants.

	Reference Case	I.I.		E	
Variation		+5%	-5%	+5%	-5%
LCOE SPT	169.6	177.2	162.0	161.7	178.4
LCOE PT	220.4	230.5	209.9	209.9	231.5
LCOE SPT variation (%)	-	4.5	-4.5	-4.7	5.2
LCOE PT variation (%)	-	4.6	-4.7	-4.7	5.0

3.4. Energy performance

The final electricity consumption in Uruguay in 2019 ascends to 973.1$ktep$ (11.32TWh) [8]. Table 14 shows the electricity generation prediction for Solar Power Tower and Parabolic Trough optimized plants, in every location.

In the case of plants located in Salto, the optimal configurations enable the generation of energy that accounts for 4.4% and 2.0% of the total yearly electricity demand. This substantial amount of electricity generation for a solar project can be attributed to the inclusion of thermal storage, which allows the plant to produce power even during nighttime. The influence of the storage can be observed in the capacity factors achieved, ranging between 47% and 59%, which are significantly higher compared to other solar technologies like photovoltaic systems with capacity factors around 18%.

In order to get further insight into the impact of the thermal storage, the daily evolution of hourly mean DNI (Figure 6) and the hourly mean gross generated power (Figs. 7 and 8) are presented for the months of January and July and for both technologies, in Salto.

Figure 7 shows that the optimized SPT plant can provide energy throughout the day in January. In July, despite having several hours of no generation, the plant continues producing significantly during the night. PT plant presents a similar behavior (see Figure 8), although with higher differences between seasons, probably due to the corresponding higher difference in optical efficiency of PT vs. SPT (see Figs. 13 and 14).

Table 14: Annual electricity generation (E) and capacity factor (CF) for the optimized plants, for each technology and location.

Location	100 MW SPT		50 MW PT	
	E (GWh)	CF (%)	E (GWh)	CF (%)
Colonia	515,1	58.8	227.8	52.0
Montevideo	469.3	53.6	221.7	50.6
Rivera	468.8	53.5	238.4	54.4
Rocha	442.4	50.5	206.1	47.1
Salto	494.4	56.4	229.0	52.3

† Note that configuration may vary between locations as presented in Tables 8 and 9.

https://www.overleaf.com/project/65ad6860607bf4e18e0b9351

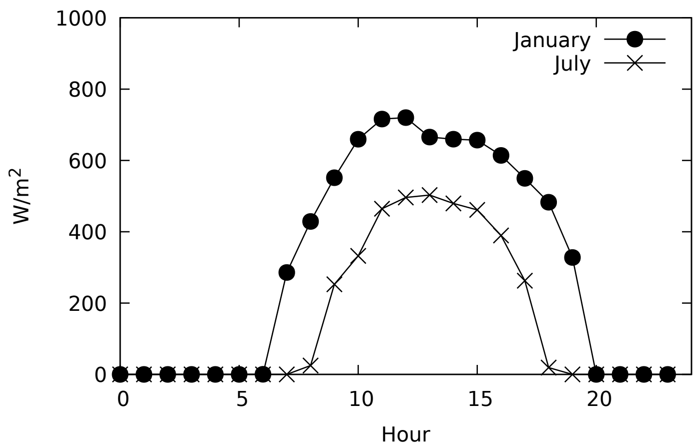

Figure 6: Mean Direct Normal Irradiation in January and July in Salto.

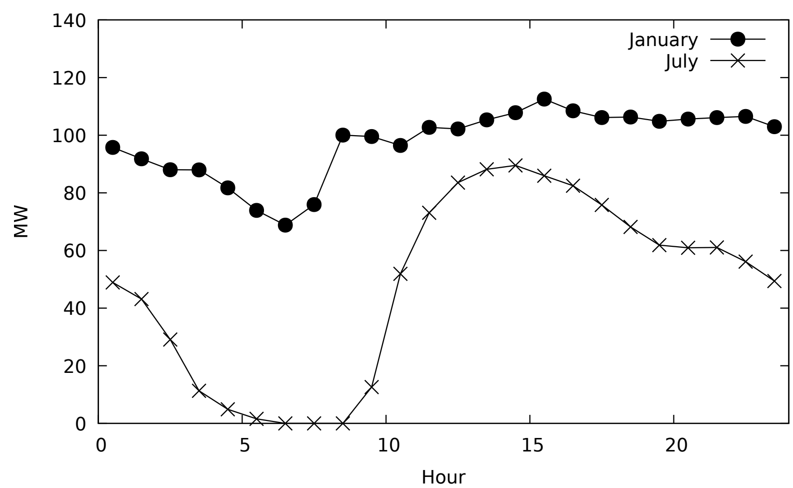

Figure 7: Mean gross power generation with SPT technology, in January and July, for the optimized plant in Salto.

To analyze the evolution of power production throughout the year, Figures 9 and 10 show the total generated electricity on a per-month basis, for both SPT and PT. Power production of the SPT plant during January, November and December nearly doubles that of winter months (May, June, July), being $55.7\,GWh$ in January and $27.6\,GWh$ in July. A similar result is observed for the PT plant, with a somewhat higher difference between seasons, being $30.7\,GWh$

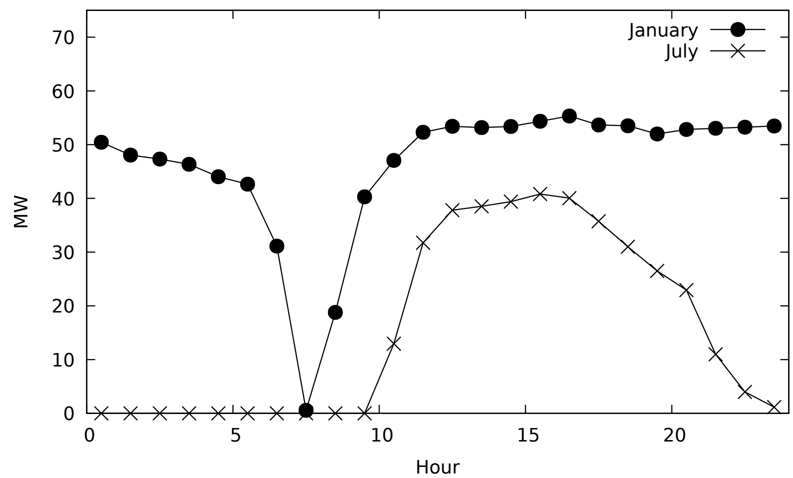

Figure 8: Mean gross power generation with PT technology, in January and July, for the optimized plant in Salto.

395 in January and 11.6 GWh in July.

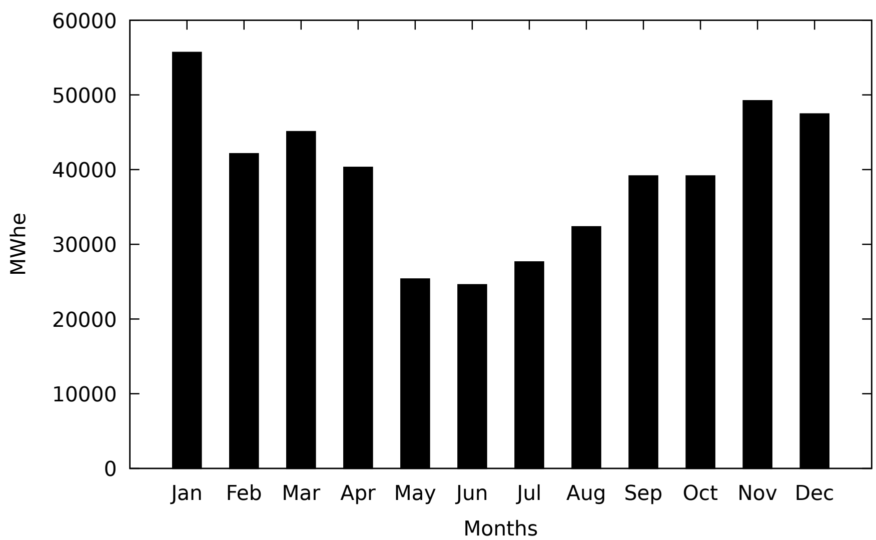

Figure 9: Monthly electricity generation with optimized 100 MW SPT plant located in Salto.

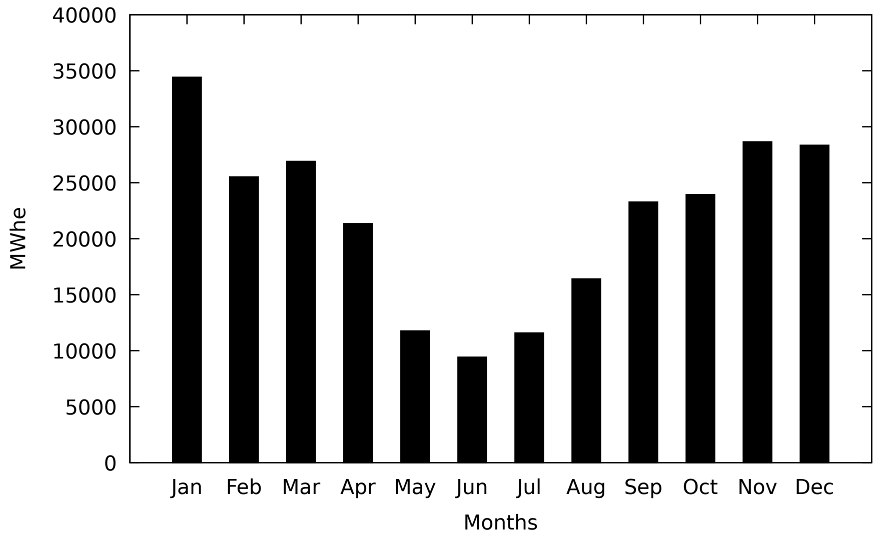

Figure 10: Monthly electricity with optimized 50 MW PT plant located in Salto.

The significance of the different losses is evaluated in order to get a better insight into the performance differences between technologies (see Figures 11 and 12). The optical efficiency represents the proportion of incident energy on the mirrors that reaches the receiver. Once the energy reaches the receiver, a portion is transferred to the heat transfer fluid (HTF), while another fraction is lost to the surrounding environment (receiver losses). The heated HTF is then directed to the heat exchanger, where steam is generated, and thermal losses occur through piping and heat exchanger walls. Additionally, losses and parasitic energy consumption associated with the Rankine cycle, such as water pump energy consumption, together with availability or curtailment losses (4% of net output), are considered.

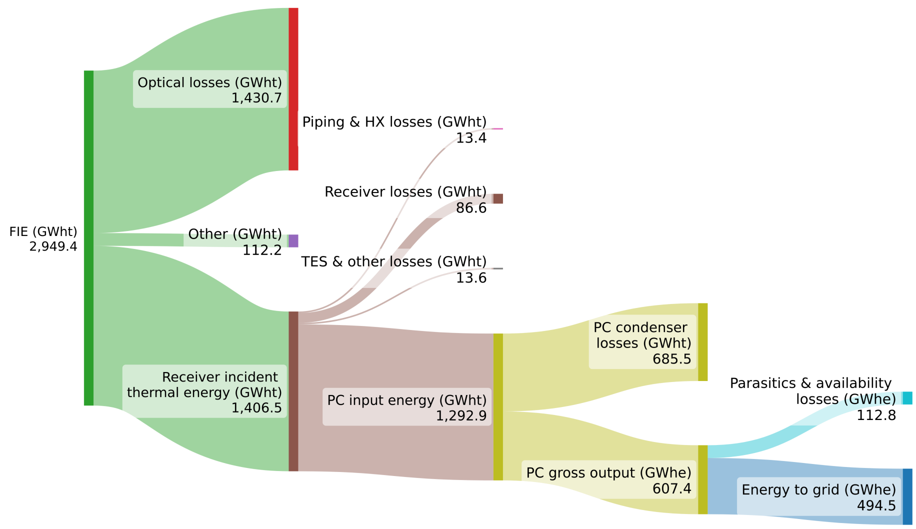

Figure 11: Energy losses of the optimized 100 MW SPT plant, located in Salto (own elaboration using [20]).

In both cases, optical losses play a predominant role, with greater significance in the SPT technology. Approximately 50% of the total incident radiation on the solar field is lost in the SPT plant, compared to 38% in PT. Additionally, there is a notable difference in the importance of receiver, piping, and heat exchanger losses, with SPT accounting for 3.6% of the total incident energy and PT showing a higher value of 15.7%. This is due to the much lower heat transfer area of the SPT "point" receiver compared to that of the PT "line focus" absorbers. It is in the power cycle where the second higher source of losses occurs (thermal losses, indicated as "PC condenser losses" in Figures 11 and 12), where around 23% and 26% of the field incident thermal power is lost, corresponding to 38.2% and 32.7% power cycle final efficiency, for SPT and PT, respectively.

Figures 13 and 14 show the hourly evolution of the mean optical efficiency for the months of January (summer) and July (winter). Significant differences are observed for both technologies, but they are higher for PT. In both cases,

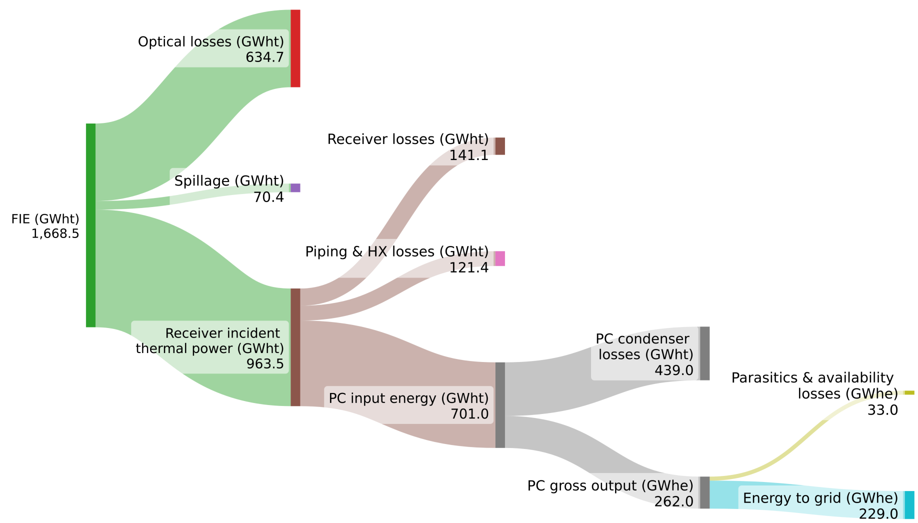

Figure 12: Energy losses of the optimized 50 MW PT plant, located in Salto (own elaboration using [20]).

higher angles of incidence of radiation on the mirrors during winter result in lower efficiencies [31, 11]. As was previously observed, this results in higher differences in power production between seasons for the PT plant.

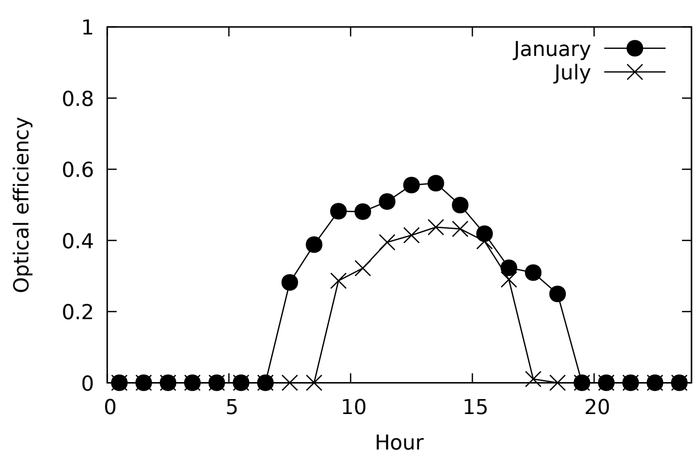

Figure 13: Optical efficiency of Solar Power Tower in Salto.

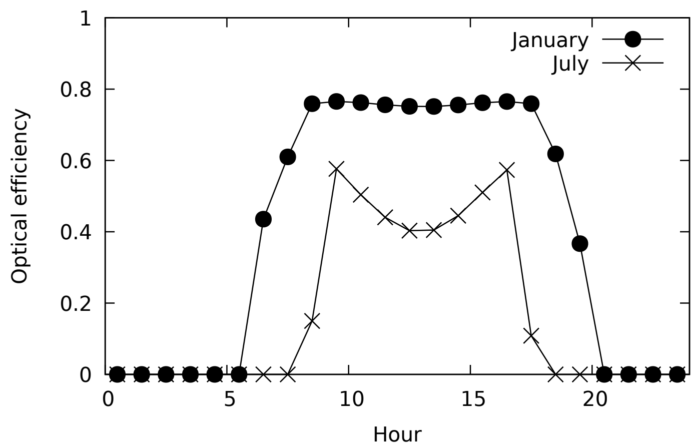

Figure 14: Optical efficiency of Parabolic Trough in Salto.

Finally, the location effect is analyzed by simulating the same plant (optimized plant for Salto), in the different locations where the TMY is available. The annual generated energy and optical efficiency are presented in Table 15 for every location. It can be observed that in Uruguay, the optical efficiency can be considered to be almost independent on the location. Regarding energy production, a difference of around 10% for both SPT and PT plants is observed between Salto (northern, hotter) and Rocha (south-eastern, colder), which is similar to the difference in LCOE.

Table 15: Annual energy (E) and optical efficiency (OE) for each technology and location.

Location	Irradiance (kWh/m^2yr)	100 MW SPT		50 MW PT	
		E GWh_e	OE (%)	E GWh_e	OE (%)
Colonia	1890.3	515.1	49.5	227.8	60.2
Montevideo	1862.5	469.3	50.8	221.7	61.0
Rivera	1779.7	468.8	52.4	212.3	60.0
Rocha	1740.6	442.4	51.4	206.1	60.0
Salto	1897.5	494.4	51.5	229.0	62.0

4. Conclusions

The current work focuses on the optimization of Solar Power Tower (SPT) and Parabolic Trough (PT) plants in different locations within Uruguay, which is a South American country with a humid subtropical climate.

System Advisor Model (SAM [23]) SPT and PT models were used and compared against results from a previous work [29]. For PT the comparison was made also against an in-house code. In all cases, a very good agreement was found (maximum variation of 2% in the annual produced energy).

An extensive search for cost data was performed. A great difference in initial investment cost values was observed between China projects and those in the rest of the world. Therefore, two sets of cost data were considered for the economic analysis. The employed initial investment cost for the least favorable scenario was $6.5\frac{MUSD}{MW}$ and $7.9\frac{MUSD}{MW}$ for $100MW$ SPT and $50MW$ PT plants, respectively. In the most favorable scenario, $5.0\frac{MUSD}{MW}$ and $6.0\frac{MUSD}{MW}$, for SPT and PT plants, respectively.

The optimization process involved determining the optimal solar field and storage sizes for five different locations in Uruguay, with a focus on economic considerations and minimizing the LCOE. As anticipated, the northern location of Salto was demonstrated to be the most favorable for CSP projects. With the least favorable investment costs considered, LCOE values obtained there were $170\frac{USD}{MWh}$ and $220\frac{USD}{MWh}$ for 100 MW SPT and 50 MW PT plants, respectively. LCOE obtained for other locations were quite similar, being $\sim 10\%$ higher for the worst location (Rocha). When the most favorable costs were considered, LCOE for Salto was reduced to $148\frac{USD}{MWh}$ (SPT) and $169\frac{USD}{MWh}$ (PT).

It is observed that the range of the LCOE values obtained is in the lower range of those of actual projects worldwide, except in China. When comparing with results obtained by other authors, with studies located in places with better solar resources, it is observed that although lower LCOE values are reported, those obtained in this work are not the highest.

LCOE sensitivity analysis showed that the uncertainty on investment costs and on generated energy affect almost linearly the LCOE. Besides the observed uncertainty on the investment costs, the adoption of different financial parameters (discount rate, study period) as well as the incidence of taxes, are also expected to affect LCOE.

In spite of being far from competitive with respect to photovoltaic or wind technologies, they seem to be close to competing against Uruguayan fossil fuels power plants. Further reduction of costs, as well as financial leveraging strategies or differential pricing of electricity, should improve economic competitiveness.

With respect to generated energy, $494.4GWh$ of annual electricity generation is estimated for the optimized 100 MWe SPT plant for Salto, with a solar multiple of 3.6 and 15 hours of storage (leading to a 56.4% capacity factor). For the optimized 50 MWe PT plant, also in Salto, an annual electricity generation of $229.0\,GWh$ is estimated (47.5% capacity factor), with a solar multiple of 4.0 and 12.5 hours of storage. The main sources of energy losses were optical losses (49% for SPT and 38% for PT), followed by power cycle losses (23% and 26% of incident energy, for SPT and PT respectively). The most significant difference was observed in thermal losses in the receivers, piping and heat exchangers, due to the much lower heat transfer area of SPT (3% SPT vs. 15% PT). Optical losses are observed to vary significantly through seasons for both technologies, due to the effect of the higher incidence angle. This difference is higher for PT, and therefore, a higher difference in power production over seasons is observed for this technology. Almost no impact on optical efficiency is observed for the different locations evaluated.

Future studies could investigate the effects on economic outcomes by considering varying prices throughout the day, such as time-of-day tariffs. This would optimize the benefits of having a storage system in place. Additionally, the exploration of financial leveraging strategies and the analysis of hybridization with existing or new fossil fuel or biomass plants could be pursued to further enhance the understanding of these technologies.

As technological evolution results in lowering costs, and with the increase of attractiveness of thermal storage, increasing competitiveness of CSP can be expected in the near future.

Acknowledgements

Authors acknowledge financial support from Agencia Nacional de Investigación e Innovación (ANII); "Fondo Sectorial de Energía", Uruguay; contract FSE-1-2015-110011. A.G. also acknowledges financial support from ANII, through its program "Programa de Becas de Posgrados Nacionales"(Ref. POS NAC 2018 1 152077).

Likewise, the authors would like to acknowledge Santiago Martínez Boggio for his invaluable contribution to manuscript editing.

References

[1] ADME (2020). Informe anual 2019. Technical report, Administración del Mercado Eléctrico. https://adme.com.uy/db-docs/Docs_secciones/nid_526/Informe_Anual_2019.pdf.

[2] Alonso, R., M. Bidegain, G. Abal, and P. Modernell (2016). Año Meteorológico Típico para aplicaciones de energía solar - AMTUes series horarias típicas para 5 sitios del Uruguay. Version 2.4. Technical report, Laboratorio de Energía Solar, UdelaR, Uruguay. https://hdl.handle.net/20.500.12008/42397.

[3] Alsagri, A. S., A. Chiasson, and M. Gadalla (2019). Viability Assessment of a Concentrated Solar Power Tower With a Supercritical CO2 Brayton Cycle Power Plant. *Journal of Solar Energy Engineering 141*(5), 051006. https://doi.org/10.1115/1.4043515.

[4] Aly, A., A. Bernardos, C. M. Fernandez-Peruchena, S. S. Jensen, and A. B. Pedersen (2019). Is concentrated solar power (CSP) a feasible option for sub-saharan africa?: Investigating the techno-economic feasibility of CSP in tanzania. *Renewable Energy 135*, 1224–1240. https://doi.org/10.1016/j.renene.2018.09.065.

[5] Biboum, A. C. and A. Yilanci (2021). Thermodynamic and Economic Assessment of Solar Thermal Power Plants for Cameroon. *Journal of Solar Energy Engineering 143*(4), 041004. https://doi.org/10.1115/1.4049066.

[6] Boretti, A. (2018). Cost and production of solar thermal and solar photovoltaics power plants in the united states. *Renewable Energy Focus 26*, 93–99. https://doi.org/10.1016/j.ref.2018.07.002.

[7] Boukelia, T., M. Mecibah, B. Kumar, and K. Reddy (2015). Optimization, selection and feasibility study of solar parabolic trough power plants for algerian conditions. *Energy Conversion and Management 101*, 450–459. https://doi.org/10.1016/j.enconman.2015.05.067.

[8] DNE (2020). Balance energético nacional. Technical report, Dirección Nacional de Energía, Ministerio de Industria y Energía, Uruguay. https://ben.miem.gub.uy/descargas/1balance/1-1-Libro-BEN2020.pdf.

[9] Dos Santos, M. P., L. H. M. Leite, and A. da Silva Reis (2017). Concentrated solar power: Analysis of economic aspects in brazil. In *2017 IEEE PES Innovative Smart Grid Technologies Conference - Latin America (ISGT Latin America)*, pp. 1–6. Quito, Ecuador, September 2017. https://doi.org/10.1109/ISGT-LA.2017.8126691.

[10] Elfeky, K. and Q. Wang (2023). Techno-economic assessment and optimization of the performance of solar power tower plant in egypt's climate conditions. *Energy Conversion and Management 280*, 116829. https://doi.org/10.1016/j.enconman.2023.116829.

[11] Ghazarian, A. (2021). Evaluation of Concentrating Solar Power for their application in Uruguay. Master's thesis, Facultad de Ingeniería, Universidad de la República, Uruguay, https://www.colibri.udelar.edu.uy/jspui/bitstream/20.500.12008/29839/1/GAH21.pdf.

[12] Ghodbane, M., E. Bellos, Z. Said, B. Boumeddane, A. Khechekhouche, M. Sheikholeslami, and Z. M. Ali (2021). Energy, Financial, and Environ-

mental Investigation of a Direct Steam Production Power Plant Driven by Linear Fresnel Solar Reflectors. *Journal of Solar Energy Engineering 143*(2), 021008. https://doi.org/10.1115/1.4048158.

[13] Ho, C. K. (2008). Software and codes for analysis of concentrating solar power technologies. sandia report sand2008-8053. Technical report, Sandia National Laboratories. https://energy.sandia.gov/wp-content/gallery/uploads/SAND2008-8053.pdf.

[14] IRENA (2019). Renewable power generation costs in 2018. Technical report, International Renewable Energy Agency, Abu Dhabi. https://www.irena.org/-/media/Files/IRENA/Agency/Publication/2019/May/IRENA_Renewable-Power-Generations-Costs-in-2018.pdf?rev=7a3b6ab611bd41ab9ec399d2e70eaa31.

[15] IRENA (2020). Renewable power generation costs in 2019. Technical report, International Renewable Energy Agency, Abu Dhabi. https://www.irena.org/-/media/Files/IRENA/Agency/Publication/2020/Jun/IRENA_Power_Generation_Costs_2019.pdf?rev=77ebbae10ca34ef98909a59e39470906.

[16] IRENA (2022). Renewable power generation costs in 2021. Technical report, International Renewable Energy Agency, Abu Dhabi. ISBN: 978-92-9260-452-3. https://www.irena.org/-/media/Files/IRENA/Agency/Publication/2022/Jul/IRENA_Power_Generation_Costs_2021.pdf?rev=34c22a4b244d434da0accde7de7c73d8.

[17] Islam, M. T., N. Huda, A. Abdullah, and R. Saidur (2018). A comprehensive review of state-of-the-art concentrating solar power (CSP) technologies: Current status and research trends. *Renewable and Sustainable Energy Reviews 91*, 987–1018. https://doi.org/10.1016/j.rser.2018.04.097.

[18] Kulichenko, N. and A. Khanna (2013). Development of local supply chain (vol. 2): The missing link for concentrated solar power projects

in india. Rep. No. 81536. Technical report, Energy Sector Management assistance Program (ESMAP) Washington, D.C.: World Bank Group. http://documents.worldbank.org/curated/en/758361468041467642/The-missing-link-for-concentrated-solar-power-projects-in-India.

[19] Ling-zhi, R., Z. Xin-gang, Z. Yu-zhuo, and L. Yan-bin (2018). The economic performance of concentrated solar power industry in china. *Journal of Cleaner Production 205*, 799–813. https://doi.org/10.1016/j.jclepro.2018.09.110.

[20] Mauri, M., T. Elli, G. Caviglia, G. Uboldi, and M. Azzi (2017). Rawgraphs: A visualisation platform to create open outputs. In *Proceedings of the 12th Biannual Conference on Italian SIGCHI Chapter*, CHItaly '17, New York, NY, USA. Association for Computing Machinery. https://doi.org/10.1145/3125571.3125585.

[21] Nadav, S. (2018). "CSP capex costs fall by almost half as developers shift towards China and Middle East". *Reuters Events. Renewables*. https://www.reutersevents.com/renewables/csp-today/csp-capex-costs-fall-almost-half-developers-shift-towards-china-and-middle-east.

[22] National Renewable Energy Laboratory. Golden, CO. Concentrating solar power projects. https://solarpaces.nrel.gov/.

[23] National Renewable Energy Laboratory. Golden, CO. (2017a). System Advisor Model Version 2017.1.17 (SAM 2017.1.17). https://sam.nrel.gov/.

[24] National Renewable Energy Laboratory. Golden, CO. (2017b). System Advisor Model Version 2017.1.17 (SAM 2017.1.17) User Documentation. https://sam.nrel.gov/.

[25] Praveen, R. P., M. Baseer, and N. Sankara (2018). Design. Performance Analysis and Optimization of a 100 MW Concentrated Solar Power Plant with Thermal Energy Storage. *Proceedings of the 2018 International Conference*

on Current Trends towards Converging Technologies, ICCTCT 2018, 1–6. https://doi.org/10.1109/ICCTCT.2018.8551033.

[26] REN21 (2019). Renewables 2019 Global Status Report. Technical report, REN21 Secretariat, Paris. ISBN 978-3-9818911-7-1. https://www.ren21.net/wp-content/uploads/2019/05/gsr_2019_full_report_en.pdf.

[27] Santos, J. J., J. C. Palacio, A. M. Reyes, M. Carvalho, A. J. Freire, and M. A. Barone (2018). Chapter 12 - concentrating solar power. In I. Yahyaoui (Ed.), *Advances in Renewable Energies and Power Technologies*, pp. 373–402. Elsevier. https://doi.org/10.1016/B978-0-12-812959-3.00012-5.

[28] Simsek, Y., C. Mata-Torres, A. M. Guzmán, J. M. Cardemil, and R. Escobar (2018). Sensitivity and effectiveness analysis of incentives for concentrated solar power projects in chile. *Renewable Energy 129*, 214–224. https://doi.org/10.1016/j.renene.2018.06.012.

[29] Solida (2014). Análisis de pre-factibilidad para el desarrollo de energía termosolar en uruguay. sots1sots150201agme0001-02. Technical report, Solida Renewable Energies. http://www.energiasolar.gub.uy/images/Solar%20de%20Concentracion/Consultoria%20Solida%202015/informe%20%20prefactibilidad%20csp.pdf.

[30] State of Uruguay (2018). Decree 143/018, Law 16.906 "Ley de Inversiones y Promoción Industrial". IMPO, Official Information Center, Uruguay. https://www.impo.com.uy/bases/decretos/143-2018.

[31] Wagner, M. (2008). Simulation and Predictive Performance Modeling of Utility-Scale Central Receiver System Power Plants. Master's thesis, University of Winsconsin-Madison, Winsconsin (MA), U.S.

[32] Wagner, M. J. and P. Gilman (2011). Technical manual for the SAM physical trough model. NREL/TP-5500-51825. Technical report, National Renewable Energy Laboratory (NREL, U.S. Department of Energy). https://doi.org/10.2172/1016437.

[33] Yang, S., X. Zhu, and W. Guo (2018). Cost-Benefit Analysis for the Concentrated Solar Power in China. *Journal of Electrical and Computer Engineering 2018*. Article ID 4063691. https://doi.org/10.1155/2018/4063691.

Appendix

Cost estimation

An extensive literature review was performed, leading to different initial investment costs which are presented in Tables 16 to 21 discriminated by installed capacity and technology. Tables 16 to 18 show information on SPT technologies of 55MW, 110 MW, and unknown installed capacity, respectively. Tables 19 to 21 present the same information for PT technology. Other relevant aspects such as the project location, available irradiation in the considered zone and storage size are also specified.

Tables 22 and 23 show information on initial investment for plants installed in the USA and Spain, respectively, together with information on storage, capacity, technology and production start date.

Finally, Tables 24 and 25 present detailed information on costs of PT and SPT plants, respectively, with specific data obtained from [23].

Table 16: Solar Power Tower 50 MW initial investment(I.I.) costs.

Solar Power Tower				
I.I. (MUSD/MW)	DNI (kWh/year)	Storage (hours)	Country	Reference (year)
50 MW				
5.1	1800	9	China	[33] (2018)
3.0-3.5	1976	6	China	[33]-[19] (2018)
3.5	1900	6	China	[33] (2018)
4.5-5.29	1870	8	China	[33]-[19] (2018)
3.9	1870	6	China	[21] (2018)
5.0	1869	8	China	[21] (2018)
6.0	1800	9	China	[19] (2018)
5.3	1600	12	China	[19] (2018)

Table 17: Solar Power Tower 100 MW initial investment (I.I.) costs.

Solar Power Tower				
I.I. (MUSD/MW)	DNI (kWh/year)	Storage (hours)	Country	Reference (year)
100 MW				
4.3	1800	10	China	[33] (2018)
4.4	2000	11	China	[33] (2018)
3.6	1900	8	China	[33] (2018)
4.0	1633	8	China	[21] (2018)
4.9	1633	11	China	[21] (2018)
5.1	2000	11	China	[19] (2018)
4.2	1900	8	China	[19] (2018)
5.0	1800	10	China	[19] (2018)
9.2	-	14	Chile	[28] (2018)
6.7	-	10	Salto	[29] (2014)

Table 18: Solar Power Tower unknown capacity initial investment (I.I.) costs.

Solar Power Tower		
I.I. (MUSD/MW)	Storage (hours)	Reference (year)
Unknown capacity and location		
7.3	7.5	[27] (2018)
6.3	6	[27] (2018)
7.4	9	[27] (2018)
7.5	6	[27] (2018)
7.7	9	[27] (2018)
9.0	12	[27] (2018)
10.5	15	[27] (2018)

Table 19: Parabolic Trough 50MW initial investment (I.I.) cost.

Parabolic Trough				
I.I. (MUSD/MW)	DNI (kWh/year)	Storage (hours)	Country	Reference (year)
50 MW				
5.7	2057	11	China	[33] (2018)
4.3	1800	9	China	[21] (2018)
6.2	1904	9	China	[21] (2018)
6.4	1733	15	China	[21] (2018)
4.5	1878	9	China	[19] (2018)
6.5	1976	9	China	[19] (2018)
9.0	-	6	India	[18] (2013)
5.8	-	0	India	[18] (2013)
6.1	-	7.5	Salto	[29] (2014)

Table 20: Parabolic Trough 100MW initial investment (I.I.) cost.

Parabolic Trough				
I.I. (MUSD/MW)	DNI (kWh/year)	Storage (hours)	Country	Reference (year)
100 MW				
4.5	1851	10	China	[21] (2018)
4.7	2025	10	China	[19] (2018)
7.9	-	14	Chile	[28] (2018)

Table 21: Parabolic Trough unknown capacity initial investment (I.I.) costs.

Parabolic Trough		
I.I. (MUSD/MW)	Storage (hours)	Reference (year)
Unknown capacity and location		
4.6	No	[27] (2018)
7.1	No	[27] (2018)
8.0	6.0	[27] (2018)
9.0	6.3	[27] (2018)
7.7	6	[27] (2018)
7.4	4.5	[27] (2018)
7.6	9	[27] (2018)
9.1	13.4	[27] (2018)

Table 22: USA CSP power plants initial investment [6]

	Start of production	Technology	Storage	Nameplate Capacity MW	I.I. (MUSD/MW)
ISEGS	Jan-14	ST	No	377	6.084
Solana	Oct-13	PT	Yes	250	8.258
Genesis	Mar-14	PT	No	250	5.213
Mojave Solar Project	Dec-14	PT	No	250	6.672
Crescent Dunes	Nov-15	ST	Yes	110	9.227

Table 23: Spain CSP power plants initial investment [22]

	Start of production	Technology	Storage	Nameplate capacity MW	I.I. (M €/MW)
Andasol 3	Aug-11	PT	7.5	50	6.3
Arcosol 50	Dec-11	PT	7.5	50	5.4
Borges Termosolar	Dec-12	PT	7.5	22.5	6.8
Gemasolar	Apr-11	SPT	15	20	11.5
Ibersol	09	PT	No	50	6.3
La Africana	Nov-12	PT	7.5	50	7.7
Moron	May-12	PT	No	50	5.9
Olivenza	Sep-12	PT	No	50	5.7
Orellana	Aug-12	PT	No	50	4.8

Table 24: Costs of a Solar Power Tower plant. Specific costs were obtained from [23]. Values of CAPEX, OPEX and I.I. correspond to a 110 MWe gross power plant, with 25,383 heliostats and 15 hours of storage.

Solar Power Tower	
Land improvement	16 (USD/m^2)
Tower fixed cost	3E6 (USD)
Tower factor	0.0113
Reference receiver cost	103.6E6(USD)
Reference receiver Area	$1571 m^2$
Receiver factor	0.7
Solar Field	145 (USD/m^2)
Storage	24(USD/MWht)
Power plant	1100 (USD/kW)
BOP†	340(USD/kW)
Land	10000 (USD/acre)
Fixed O&M‡	66(USD/kW-año)
Variable O&M	3.5(USD/MWh)
Contingency cost	7% of total cost
CAPEX (MUSD)△	718.5
OPEX(MUSD/year)▽	8.99
I.I. (MUSD/MW)	6.5

† Balance Of Plant (auxiliary systems)
‡ Operation and Maintenance
△ Capital Expenditures (e.g. machinery, equipment)
▽ Operating Expenditures (e.g. salaries)

Table 25: Costs of Parabolic Trough plant. Specific costs were obtained from [23]. Values of CAPEX, OPEX and I.I. correspond to a 55MWe gross power plant, with 254 loops and 12.5 hours of storage.

Parabolic Trough	
Land improvement	25 (USD/m^2)
Solar Field	150 (USD/m^2)
HTF$^\diamond$ system	60 (USD/$\mathbf{m^2}$)
Storage	65(USD/MWht)
Power plant	1150 (USD/kW)
BOP	120(USD/kW)
Land	10000 (USD/acre)
Fixed O&M‡	66(USD/kW-año)
Variable O&M	4(USD/MWh)
Contingency cost	7% of total cost
CAPEX$^\triangle$ (MUSD)	433.8
OPEX(MUSD/year)$^\triangledown$	4.5
I.I. (MUSD/MW)	7.9

† Balance Of Plant (auxiliary systems)
‡ Operation and Maintenance
$^\triangle$ Capital Expenditures (e.g. machinery, equipment)
$^\triangledown$ Operating Expenditures (e.g. salaries)
$^\diamond$ Heat Transfer Fluid